

Link-Level Performance Evaluation of Sidelink Synchronization Signal Block for 5G V2X

Daegun Jang
dept. ICT Convergence
Soonchunhyang University
Asan, Republic of Korea
wowhensum@sch.ac.kr

Subin Jo
dept. Information and Communication
Engineering
Soonchunhyang University
Asan, Republic of Korea
0909subin@naver.com

Gayeon Kim
dept. Information and Communication
Engineering
Soonchunhyang University
Asan, Republic of Korea
bobo4131@sch.ac.kr

Jeonghoon Bae
dept. Information and Communication
Engineering
Soonchunhyang University
Asan, Republic of Korea
albert1022@sch.ac.kr

Taejun Choi
dept. Information and Communication
Engineering
Soonchunhyang University
Asan, Republic of Korea
20184123@sch.ac.kr

Taehyoung Kim
dept. Information and Communication
Engineering
Soonchunhyang University
Asan, Republic of Korea
th.kim@sch.ac.kr

Abstract— In this paper, we evaluate the performance of sidelink synchronization signal block (SL-SSB) for 5G vehicular-to-everything (V2X) communication systems. The SL-SSB serves to establish communication link by synchronizing signals between the vehicles. We first introduce the transmission structure of SL-SSB and related synchronization procedures based on the standard documents presented by 3rd Generation Partnership Project (3GPP). Then, we develop a link level simulator (LLS), and evaluate the SL identity (ID) detection performance based on the SL-SSB and block error rate (BLER) performance for the physical sidelink broadcast channel (PSBCH).

Keywords—V2X, sidelink, SL-SSB, SL-PSS, SL-SSS, PSBCH

I. INTRODUCTION

There has been a lot of interest and investment in autonomous driving technology recently, and as a result, research and development in this area are also actively underway. In particular, vehicle-to-everything (V2X) technology, which refers to communication between vehicles and everything else, is gaining attention. V2X technology encompasses vehicle-to-pedestrian (V2P) for communication between vehicles and pedestrians, vehicle-to-network (V2N) for communication between vehicles and networks, and vehicle-to-vehicle (V2V) for communication between vehicles. sidelink (SL) technology was introduced for communication between vehicles, allowing different vehicles to exchange information without the intervention of gNodeB (gNB). This has the advantage of allowing communication between vehicles even outside the network coverage of gNB, and an example of this is shown in Fig. 1. In the SL system, the transmitting user equipment (UE) periodically sends a sidelink synchronization signal block (SL-SSB), and the receiving UE can obtain the sidelink identity (SLID) required for frame synchronization and SL connection by monitoring it [1]. The SL-SSB is composed of the sidelink primary synchronization signal (SL-PSS), sidelink secondary synchronization signal (SL-SSS), physical sidelink broadcast channel (PSBCH), and demodulation reference signal (DMRS), and the DMRS is transmitted together inside the PSBCH [1], [3]. The SL-PSS is the first synchronization signal that the receiving UE searches for, and one of the two m-sequences is selected and mapped according to the frame

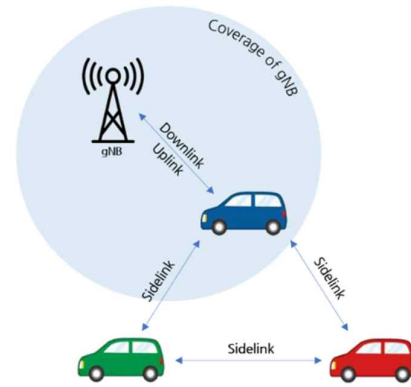


Fig. 1. Illustration of 5G V2X networks.

structure of the SL-SSB. Which of the two SL-PSS sequences to use is determined by the SLID [2]. Since the receiving UE does not know which SL-PSS sequence the transmitting UE used, it calculates the correlation between the received SL-PSS and both possible SL-PSS sequences when detecting the SL-PSS, and selects the sequence with the highest correlation [1], [2]. The second synchronization signal, SL-SSS, has 336 sequences, and since the receiving UE cannot know which SL-SSS sequence the transmitting UE used, it detects the sequence with the highest correlation, as with the SL-PSS detection. The receiving UE that detects SL-PSS and SL-SSS can detect the corresponding SLID among 672 SLIDs by combining them. The detected SLID through this process is used for PSBCH decoding [1], [2]. The UE that performs PSBCH decoding can acquire the master information block (MIB) corresponding to the SL system information it wants to connect to.

In this paper, we introduce the SL-SSB, which is the basis of SL, and analyze its transmission structure. We build a link level simulator (LLS) to measure the SLID detection performance and PSBCH block error rate (BLER) performance in a tapped-delay line D (TDL-D) channel environment, and evaluate the performance of SL-SSB according to changes in Signal-to-Noise Ratio (SNR).

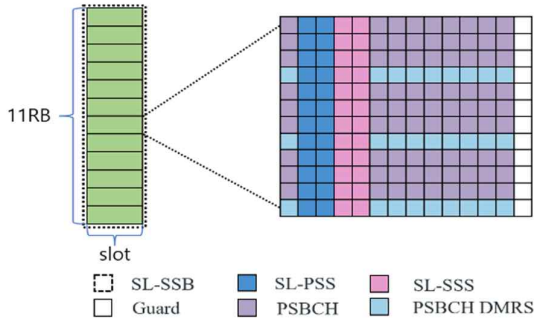


Fig. 2. SL-SSB frame structure.

II. SL-SSB FRAME STRUCTURE

A. SL-PSS/SSS structures

As the first procedure of the initial access phase in SL, the SL-SSB is transmitted. SL-SSB consists of SL-PSS, SL-SSS, PSBCH, and DMRS, and the frame structure of SL-SSB is illustrated in Fig. 2.

SL-SSB is transmitted every 160ms and consists of 14 orthogonal frequency division multiplexing (OFDM) symbols on the time axis, with the last symbol composed of guard symbols. The SL-PSS is transmitted in the 2nd and 3rd symbols, with 127 subcarriers allocated for each symbol on the frequency axis. The SL-PSS sequence d_{SL-PSS} is generated as

$$d_{SL-PSS}(n) = 1 - 2x(m), \quad (1)$$

where $m = (n + 22 + 43 \frac{N_{D,2}^{SL}}{2}) \bmod 127$, $x(i+7) = (x(i+4) + (x(i)) \bmod 2) \bmod 127$. $m \bmod$ is modulo operation. $0 \leq n < 127$ represents the index of the subcarrier to the SL-PSS symbol. $N_{D,2}^{SL}$ has a value of 0 or 1, indicating the number of the SL-PSS sequence. The sequence x is extended from an initial value of $[x(6) \ x(5) \ \dots \ x(0)] = [1 \ 1 \ 1 \ 0 \ 1 \ 1 \ 0]$ based on its index in the SL-PSS sequence according to (1) [3]. The SL-PSS generated by this process is a binary phase shift keying (BPSK) signal, which is assigned to subcarriers as shown in Fig. 2.

In the 4th and 5th symbols, SL-SSS is transmitted, with subcarriers allocated in the same way as SL-PSS. SL-PSS and SL-SSS together define the sidelink synchronization signal (SL-SS), which is assigned to subcarriers 3 to 129 out of 132 subcarriers. The sequence d_{SL-SSS} for SL-SSS is generated as

$$d_{SL-SSS}(n) = [1 - 2x_0((n + m_0) \bmod 127)] \cdot [1 - 2x_1((n + m_1) \bmod 127)], \quad (2)$$

where $m_0 = 15 \left\lfloor \frac{N_{D,1}^{SL}}{112} \right\rfloor + 5N_{D,2}^{SL}$, $m_1 = N_{D,1}^{SL} \bmod 112$, the variable x_0 is expanded based on the index i of the SL-SSS sequence from the initial value $[x_0(6) \ x_0(5) \ \dots \ x_0(0)] = [0 \ 0 \ 0 \ 0 \ 0 \ 1]$. Similarly, x_1 has the same initial value and is expanded by i to become $x_1(i+7) = (x_1(i+1) + (x_1(i)) \bmod 2) \bmod 127$. The variable n represents the subcarrier index where the SL-SSS symbol is allocated, and $N_{D,1}^{SL}$ takes on values from 0 to 335 to represent the sequence number of the SL-SSS [2], [3]. The SLID, $N_{D,1}^{SL}$, can be determined by combining $N_{D,1}^{SL}$ and $N_{D,2}^{SL}$ and is determined as

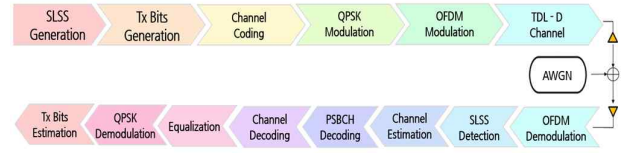


Fig. 3. Block diagram for LLS.

TABLE I. SIMULATION PARAMETERS.

Parameter	Value
SLID	17
Carrier frequency	6 [GHz]
Subcarrier spacing	30 [KHz]
Channel	TDL-D
FFT size	2048
Samplerate	61,440,000
Delayspread	10, 30 [ns]
Speed of vehicle	30, 100 [km/h]
Noise	AWGN
Channel coding	Polar coding
Equalization	MMSE
SNR	-15:1:-9, -6:2:10 [dB]
Iteration	100,000

$$N_D^{SL} = N_{D,1}^{SL} + 336N_{D,2}^{SL}. \quad (3)$$

The UE that received the SL-SSB starts SLID detection. This involves calculating the correlation between all sequences of the received SL-PSS and SL-SSS and selecting the sequence with the highest correlation to detect SL-PSS and SL-SSS as

$$i_{SL-SS}^* = \arg \max \left| \sum_{k=0}^{L-1} \{r_{S-SS}[k] \cdot x_{S-SS,i_{SL-SS}}[k]\} \right|^2, \quad (4)$$

where $S-SS$ refers to SL-SS, and k represents the subcarrier index to which the sequence is assigned [2]. L is the sequence length of SL-SS. Additionally, i_{SL-SS} indicates the sequence number of SL-PSS and SL-SSS [2].

B. PSBCH structure

Except for the guard symbol and SL-SS in the SL-SSB, the remaining OFDM symbols transmit PSBCH and DMRS, which are allocated and transmitted as shown in Fig. 2. DMRS is allocated to the positions corresponding to $4n(0 \leq n \leq 32)$ out of 132 subcarriers per symbol transmitted, and is generated as

$$r(m) = \frac{1}{\sqrt{2}}(1 - 2c(2m)) + j \frac{1}{\sqrt{2}}(1 - 2c(2m+1)), \quad (5)$$

where $r(m)$ denotes DMRS, and c represents the Pseudo-random sequence. The m -sequence used in generating c is initialized with N_D^{SL} , and is generated thereafter. m takes integer values from 0 to 296 according to the frame structure shown in Fig. 2. DMRS generated based on (5) is used for channel estimation. PSBCH contains information such as a 1-bit in coverage indicator, 10-bit direct frame number (DFN), 12-bit Indication of time division duplex (TDD) configuration,

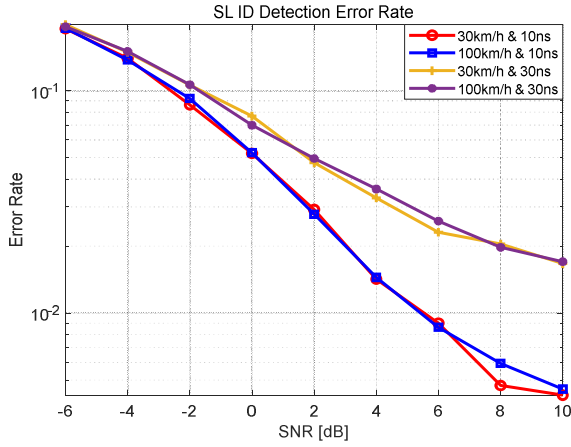


Fig. 4. SLID detection performance according to vehicle speed and delay spread difference.

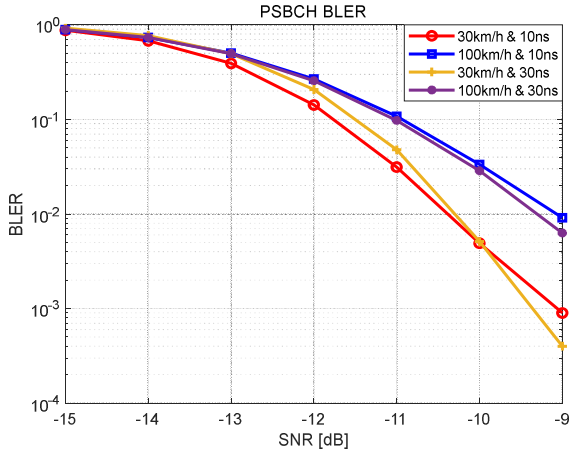


Fig. 5. PSBCH BLER performance according to vehicle speed and delay spread difference.

12-bit slot index, 24-bit cyclic redundancy check (CRC), and 2-bit reserved bits, among others [4], [5]. The above information is channel coded, and then generated into a codeword, which is scrambled as

$$\tilde{b} = (b(i) + c(i)) \bmod 2, \quad (6)$$

where \tilde{b} is the scrambled codeword, and b is the codeword before scrambling, i is the index of each codeword, and c is the Pseudo-random sequence initialized with N_D^{SL} as in (5). After scrambling, the resulting codeword is quadrature phase shift keying (QPSK) modulated and allocated on the time and frequency axes, and transmitted via OFDM modulation. Upon receiving the SL-SSB, the UE performs SLID detection, channel estimation through DMRS, and equalization and QPSK demodulation of the PSBCH symbol. Subsequently, the PSBCH symbol is descrambled and channel decoded to obtain synchronization information [5].

III. SIMULATION RESULTS

Based on the described content, we constructed an LLS to evaluate the SLID detection performance and PSBCH BLER performance using SL-PSS and SL-SSS. The SLID detection simulation was conducted under the assumption of ideal frequency synchronization between the transmitter and receiver to simplify the process. PSBCH BLER was executed

assuming accurate detection of SLID. Both simulations varied the vehicle speed and delay spread, the overall simulation configuration diagram is the same as Fig. 3. And the simulation parameters are shown in Table 1 [5].

Fig. 4. compares the SLID detection performance based on vehicle speed and delay spread. As shown in the graph, we can observe that the SLID detection error rate decreases as the signal-to-noise ratio (SNR) increases, and regardless of vehicle speed (30km/h, 100km/h), better performance is observed when the delay spread is 10ns rather than 30ns. Therefore, the delay spread has a greater impact on SLID detection performance, and a smaller delay spread results in better detection performance.

Fig. 5. shows the PSBCH BLER performance based on vehicle speed and delay spread. Similar to the SLID detection simulation, we confirmed that the PSBCH error rate decreases as the SNR increases. However, in contrast to the SLID

SLID detection performance according to vehicle speed and delay spread difference detection simulation, we observed that regardless of the delay spread (10ns, 30ns), better performance is achieved when the vehicle speed is 30km/h rather than 100km/h. Therefore, vehicle speed has a greater impact on PSBCH BLER performance, and slower vehicle speed results in better performance.

IV. CONCLUSION

This paper introduces the SL-SSB, which is transmitted as the first procedure during the initial access phase in NR V2X SL, and evaluates the performance of SLID and PSBCH using the SL-PSS, SL-SSS, PSBCH, and DMRS components of the SL-SSB. Based on the standard, an LLS for SLID and PSBCH was established, and the SLID detection and PSBCH BLER performance were evaluated in a TDL-D channel environment.

ACKNOWLEDGMENT

This work was supported by the National Research Foundation of Korea (NRF) Grant through the Korea Government [Ministry of Science and Information and Communication Technology (MSIT)] under Grant NRF-2022R1F1A1064106.

REFERENCES

- [1] M. H. C. Garcia, A. Molina-Galan, M. Boban, J. Gozalvez, B. Coll-Perales, T. Sahin, "A tutorial on 5G NR V2X communications," *IEEE commun surveys Tuts.*, vol. 23, pp. 1981-1988, Third Quarter 2021
- [2] Haesung Ahn, Hyeonseok Kim, Eunyoung Cha, and Jeongchang Kim, "Cell ID Detection Schemes Using PSS/SSS for 5G NR System," (in Korean), *JBE*, vol. 25, no. 6, pp. 870-877, Nov. 2020
- [3] TSG RAN; NR; *Physical channels and modulation (Release 17)*, document TS 38.211 V17.0.0, 3GPP, Dec. 2021
- [4] TSG RAN; NR; *Multiplexing and channel coding (Release 17)*, document TS 38.212 V17.0.0, 3GPP, Dec. 2021
- [5] TSG RAN; NR; *Physical layer procedures for control (Release 16)*, document TS 38.213 V16.9.0, 3GPP, Mar. 2021